Work-function dependence of above-surface neutralization of multicharged ions

F. W. Meyer, L. Folkerts, I. G. Hughes, S. H. Overbury, D. M. Zehner, and P. A. Zeijlmans van Emmichoven*
Oak Ridge National Laboratory, Oak Ridge, Tennessee 37831-6372

J. Burgdörfer
Oak Ridge National Laboratory, Oak Ridge, Tennessee 37831-6377
and Department of Physics, University of Tennessee, Knoxville, Tennessee 37996-1200
(Received 21 May 1993)

Measurements have been made of projectile K-Auger-electron emission during interactions of 60-keV N^{6+} ions grazingly incident on a Au(011) single crystal whose work function was modified by submonolayer deposits of Cs. K Auger spectra were obtained for incidence angles in the range 0.3°–5°, using clean, as well as cesiated, Au surfaces whose work function had been reduced by as much as 3.3 eV. For incidence angles smaller than 5°, an enhancement on the above-surface K Auger component, relative to that observed for "clean" Au, could be discerned with decreasing surface work function, which appears to saturate below 0.7° (corresponding to an inverse perpendicular velocity of about 200 a.u.$^{-1}$) at approximately 30–35 %. The experimental results are compared with modeling studies of the work-function dependence of above-surface neutralization and projectile K Auger emission, using a simulation based on the classical over-the-barrier model that was modified to treat the case of a "two-component" surface. The simulation results agree qualitatively with the experimental results up to $v_\perp^{-1}=200$. At higher inverse perpendicular velocities, the simulated enhancement continues to increase and exceeds the clean Au result by more than a factor of 2 at $v_\perp^{-1}=1000$. Speculations about possible reasons for this discrepancy will be presented.

PACS number(s): 79.20.Rf, 34.70.+e, 32.80.Dz

INTRODUCTION

The critical distance above the surface at which conduction-band electrons can start to neutralize incident multicharged projectiles by classical overbarrier transitions is inversely proportional [1] to the metal work function W. The principal quantum number n of the projectile shell into which the electrons are initially captured scales as $W^{-1/2}$. For N^{6+} ions incident on a clean Au target, this critical distance is approximately $20a_0$, and initial capture occurs into $n=7$. At the very low perpendicular velocities required to observe a contribution of above-surface neutralization [2–6] in the total projectile K-Auger-electron emission, significant projectile image-force acceleration occurs [1,5,7–9]. This places an upper limit on the above-surface interaction time, and thereby limits the observed above-surface K Auger yield [5,7] to less than about 20% of the total K Auger emission. Sufficiently close to the surface and subsequent to its penetration, screening effects facilitate direct capture into lower projectile n levels (for N projectiles $n=2-3$), leading to a filling of the surviving K-shell vacancies at an overall rate limited essentially by that of the final K Auger transition. The total K-Auger-electron emission thus arises predominantly as a result of "subsurface" processes [7,10–12]. By subsurface, we mean that region close to or below the surface where the magnitude of the electron density has reached approximately that of the target bulk. In an attempt to increase the above-surface K Auger yield, we performed measurements of K Auger spectra for N^{6+} ion impact on a cesiated Au single crystal. By varying the amount of Cs coverage between 0 and 1 monolayers, we were able to obtain a surface work-function reduction of up to about 3 eV. This change results in a more than doubling of the critical distance for over-the-barrier neutralization.

EXPERIMENTAL PROCEDURE AND RESULTS

Most of the details of the experimental apparatus and procedure used for the present measurements have been reported elsewhere [7]. To permit the measurements described here, a Cs dispenser with shutter was mounted in our experimental chamber approximately 6 cm from the single-crystal Au target. By resistive heating of the dispenser above a threshold temperature monitored by a chromel-alumel thermocouple, a reproducible flux of Cs could be obtained, to which the Au crystal could be exposed. Figure 1 shows the work-function change of the cesiated Au surface as a function of Cs exposure time. The work-function change was measured by a retarding-field method using normally incident 200-eV electrons. The relative amount of Cs deposited was monitored by electron-induced Auger spectroscopy. Although we were not able to establish directly the quantitative relation between work-function change and Cs coverage, it is known from studies of thin Cs-Au films [13] and from analogous K deposition experiments [14] on Au(110) that the work function decreases roughly monotonically as the alkali

*Present address: Department of Atomic and Interface Physics, Debye Institute, University of Utrecht, Postbus 80.000, 3508 TA Utrecht, The Netherlands.

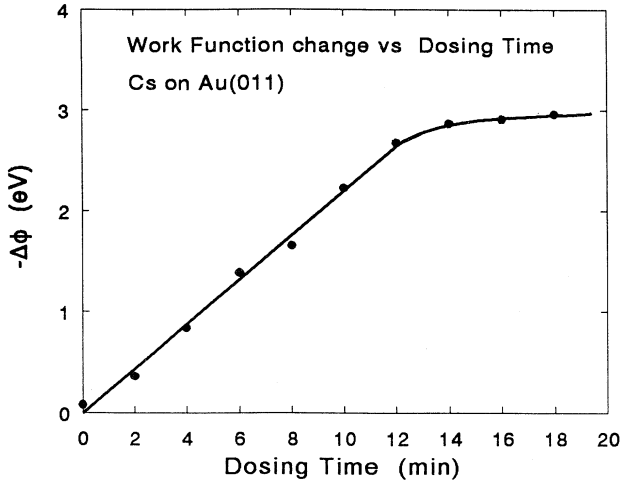

FIG. 1. Measured work-function change as a function of Cs dosing time.

metal is deposited, reaching a minimum at a coverage of roughly 0.5 monolayers, and then increases again slightly with further increasing coverage towards its equilibrium value. We thus estimate that the "knee" evident in Fig. 1 corresponds to about 0.5-monolayer Cs coverage.

Using the above procedure, projectile K Auger spectra were measured at incidence angles in the range 0.3–5° for clean and cesiated Au. The calibration of the incidence angle of the ion beam was performed in a manner described elsewhere [15]. The results are illustrated in Fig. 2. The backgrounds which have been subtracted in Fig. 2 are smoothly varying functions of electron energy (see, e.g., Fig. 5 of Ref. [7]), and contribute less than 20% of the total electron signal measured at 350 eV for the grazing angles shown in the figure. For the 1.4° and 0.7° incidence-angle measurements (top two panels of Fig. 2), as well as for the 0.5° incidence case not shown in the figure, the following procedure was used. After preparation of the Au surface by Cs dosing, the surface work-function change was determined as described above. Subsequent to acquisition of an electron spectrum at a particular incidence angle (shown in left half each panel), *in situ* thermal desorption was employed to remove the Cs overlayer, after which another electron spectrum was acquired (right half of each panel). Subsequent to this measurement the loss of Cs was confirmed by a second work-function determination. The only difference in experimental conditions between the two spectra was thus the amount of Cs coverage. While significantly reducing the Cs coverage in each case (see measured work-function changes noted in each panel), it was discovered after the fact that the thermal desorption cycles were unsuccessful in completely removing the Cs overlayer, either due to insufficiently high desorption temperatures or insufficiently long desorption times. For this reason, the spectra for the smallest incidence angle were measured in reverse order. For the 0.3° incidence angle, the electron spectrum shown on the right-hand side of the lowest panel was acquired first, immediately after sputter cleaning of the Au sample. The sample was then rotated toward the Cs dispenser, and dosed. After determination of the work-function change, the sample was returned to the initial incidence angle setting using the procedure outlined in Ref. 15 for the measurement shown in the left half of the panel.

As has been previously verified both for Au and Cu targets [7], at an incidence angle of 5° the K Auger peak arises solely from subsurface neutralization and relaxation processes. In the present measurements, the shapes of the 5° K Auger peaks were found to be independent of Cs coverage in the 0–0.7-monolayer range investigated, and were used as estimates of the subsurface components in the more grazing incidence-angle spectra. This is illustrated in Fig. 2, where the 5° background-subtracted spectra are shown for all the investigated surface conditions, scaled to have the same intensity as the grazing spectra at 380 eV, where only subsurface emission contributes, and shifted upward in energy a small amount

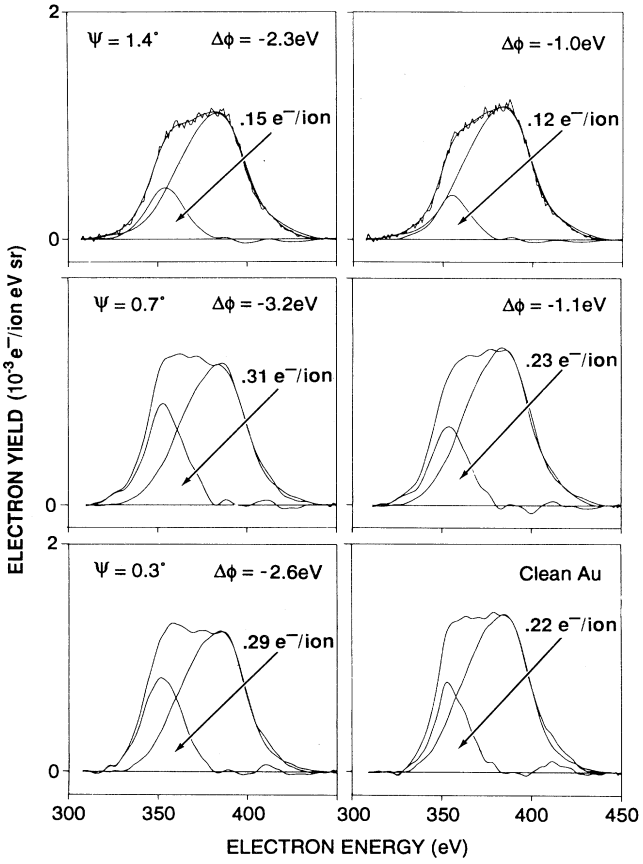

FIG. 2. Background-subtracted projectile K Auger peaks for 60-keV N^{6+} grazingly incident on cesiated and clean Au(110), together with 5° reference spectra used to estimate the subsurface components (see text); observation is perpendicular to the incident-beam direction; the difference spectra (above-surface components) and their integrated yields are also shown; for each spectrum the surface condition is specified by the work function measured relative to that of clean Au, $\Delta\Phi$. A three-point smoothing has been applied to all spectra. Representative unsmoothed spectra are shown in the top panel.

(1–2 eV) to match the high-energy portions of the grazing spectra. In using this procedure the implicit assumption is made that, even at the most grazing incidence angles, the projectiles sample the region sufficiently close to or below the surface where the electron density approaches the bulk value. At extreme grazing conditions, such interactions are more likely to occur if the single-crystal target has surface defects. Indeed, a shielded-potential approximation low-energy electron diffraction (SPA-LEED) diagnostic performed on the Au single crystal used in the present measurements indicated terrace widths of a few hundred Å, which makes it quite likely that a large fraction of the incident projectiles have an encounter with at least one step surface defect, as a result of which they can undergo closer interaction with the surface prior to reflection. Further indication of the presence of surface defects is provided by our observation of target Auger electron emission [7] for very grazing projectile incidence angles. Under such grazing conditions, the probability for close encounters necessary for inner-shell vacancy transfer was calculated [7] to be almost negligible for perfect single-crystal surfaces, but to become appreciable if surface damage is assumed.

As can be seen from the spectra shown on the right in Fig. 2, pronounced above-surface components are evident in all the grazing incidence spectra even in the case of minimal Cs coverage. Furthermore, significant enhancements of these above-surface K Auger components were observed for the reduced work-function surfaces produced by Cs deposition (spectra on left in Fig. 2).

SIMULATIONS AND DISCUSSION

For the work-function reductions indicated in Fig. 2, more than a factor of 2 increase in the above-surface critical distance should have been realized. The maximum enhancement of the above-surface K Auger yield observed at any of the investigated incidence angles due to the larger critical distances was about 35%. As noted earlier, the increase in the critical distance for first electron capture by the projectile is accompanied by an increase in the principal quantum number initially populated, due to the reduced binding energy of the neutralizing target (i.e., Cs) electrons, and the reduced upward projectile energy-level shifts due to the image-potential interaction at the larger above-surface distances. It is therefore to be expected that the subsequent de-excitation cascade populating the projectile inner shells will require more time. In addition, certainly for a thick Cs layer, the surface electron density of states at the Fermi level may be significantly reduced relative to the clean Au case, thereby reducing the number of metal electrons available for projectile neutralization. The latter two effects would tend to decrease the above-surface K-Auger-electron emission for a particular interaction time. On the other hand, since the neutralization occurs at larger distances above the surface, the image-potential acceleration of the projectile will likely be significantly reduced, which should increase the time available for the above-surface cascade and subsequent K Auger emission, and therefore increase the observed above-surface K Auger yield.

In order to quantitatively estimate the overall effect on the above-surface neutralization and subsequent K Auger emission that could be expected as a result of the factors just enumerated, simulations were carried out using a modification of the previously described [1] over-the-barrier above-surface neutralization code. Two different models for the work-function change of a cesiated metal surface were investigated. The first model is most appropriate in the limit of a "thin" adsorption layer only partially covering the substrate surface. In this model, the adsorbed Cs atoms are assumed to be surface ionized upon reaching an available surface lattice site, thereby creating a surface dipole layer which counteracts the dipole layer potential of the substrate and reduces the surface work function. The surface density of states of the substrate is assumed to be unchanged. Accordingly, cesiation only shifts the substrate band structure upward in energy by an amount equivalent to the work-function reduction.

As an alternative, we have also explored a "thick"-adlayer model in which both the band structure of the Au substrate ($\phi=5.1$ eV and $\epsilon_F=5.5$ eV) [16] and the band structure of the Cs overlayer were taken into account. The electronic band structure of the adlayer is described by a quasifree-electron-gas model. The bottom of the band is assumed to coincide with the bulk value $V_0=3.73$ eV [16]. The Fermi energy $\epsilon_F=V_0-W$ and the density of states at the Fermi edge, given by

$$D(\varepsilon_F)=\frac{\sqrt{2}}{\pi^2}(V_0-W)^{1/2}\,, \tag{1}$$

are both treated as explicit functions of the work function W.

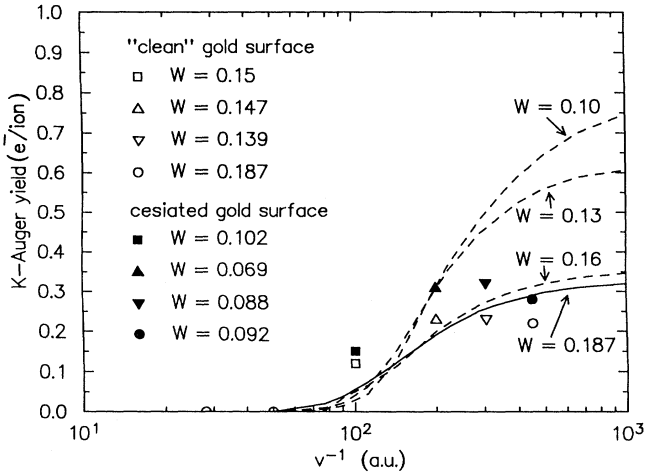

FIG. 3. Inverse perpendicular velocity dependence of the simulated above-surface K Auger yields for N^{6+} ions incident on clean and cesiated Au surfaces, for a range of surface work-function values (given in atomic units). Data points are experimentally deduced above-surface K Auger "yields" obtained for the work-function conditions identified in the figure. Relative and total uncertainties in the deduced yields are estimated to be ±20% and ±50%, respectively. Uncertainties in abscissa values are determined by the ±0.2° uncertainty in incidence angle determination (see Fig. 3 of Ref. [15]).

For a given work function and charge state, the two models give identical values for the critical distance at which the first overbarrier charge transfer takes place,

$$R_c(W) \simeq \sqrt{8q+2}/2W \ , \tag{2}$$

but differ in the resonant capture and reionization rates due to the different spectral density of states (or equivalently, the supply of electrons).

A large number of calculations were carried out, in a manner similar to that described in Ref. [1], to determine how sensitively the simulation results depended on the modeling of the adsorption layer, on the different forms of image potentials and screening functions used, and variations in the assumed Auger rates. Not surprisingly [1], the absolute magnitude of the simulated above-surface K Auger yields depended quite sensitively on the input parameters mentioned, including those describing the cesiated Au surface. Most remarkably, however, the simulation results for the *relative* yield increase as a function of decreasing perpendicular velocity were found to depend strongly only on the work function of the Cs overlayer, and not on the effective density of states.

Figure 3 shows the inverse perpendicular velocity dependence of the simulated above-surface K Auger yields for a number of different surface work functions in the range 0.1–0.187 a.u. using the "thick-layer" model [see Eq. (1)]. The other simulation parameters have been kept fixed to reproduce approximately the "upper bound" simulation results for a clean Au target (see Ref. [1] for details). Also shown in the figure are the above-surface K Auger yields deduced from the present experimental results. The experimental yields were obtained by energy integrating the difference spectra (i.e., above-surface components) shown in Fig. 2, and then multiplying the resulting angle-differential yields by 4π (i.e., assuming isotropic emission). It is emphasized that both the simulation and experimental results shown in the figure are not to be considered as direct observables, and reflect rather total K-Auger-electron *production,* irrespective of the subsequent fate of those electrons.

The simulations qualitatively reproduce the experimental data, displaying an enhancement of the K Auger production by cesiation. A comparison indicates two different trends: At higher perpendicular velocities $v_\perp > 0.005$ a.u. ($v_\perp^{-1} \leq 200$), the simulation can even quantitatively reproduce the enhancement which is quite remarkable in view of the complexity of the process. However, at extremely small perpendicular speeds ($v_\perp^{-1} > 200$) (i.e., extremely small grazing angles), the simulations predict an enhancement relative to the clean surface of more than a factor 2 while the experiment gives only an increase by a factor ≈ 1.3. The experimental results suggest a saturation in the cesiated surface results already at an inverse perpendicular velocity of about 200 a.u.$^{-1}$ while the simulation finds saturation at progressively smaller velocities as the work function decreases. This discrepancy persists for all simulations, employing a large variety of input parameters including different descriptions of the electronic structure of the Cs adlayer.

In order to elucidate the mechanism for the enhancement of K Auger production by changes of the work function, we present in Fig. 4 simulation results for the evolution of the n-shell electron populations $P(n)$ as the N^{6+} ion approaches a clean [Fig. 4(a)] and a cesiated Au surface [Fig. 4(b)] at a perpendicular velocity of 5×10^{-3} a.u. According to the overbarrier estimate [Eq. (2)], resonant electron transfer sets in much earlier and populates significantly higher n shells ($n \approx 10$ instead of 7) in the cesiated Au case. As the ion descends further toward the surface, resonant capture and loss as well as Auger deexcitation transfers the population to lower shells.

Most remarkable is the fact that by the time the projectile has approached to within $10a_0$ of the surface, the low ($n \leq 6$) n-shell population distribution for the clean Au case has almost "caught up" with the population distribution for the cesiated surface case. Therefore, contrary to what might be naively expected, the increased interaction time available for the Auger cascade resulting from the increased critical distance is *not* the dominant mechanism for the enhanced K Auger production. Slower Auger rates in the higher n shells populated first largely

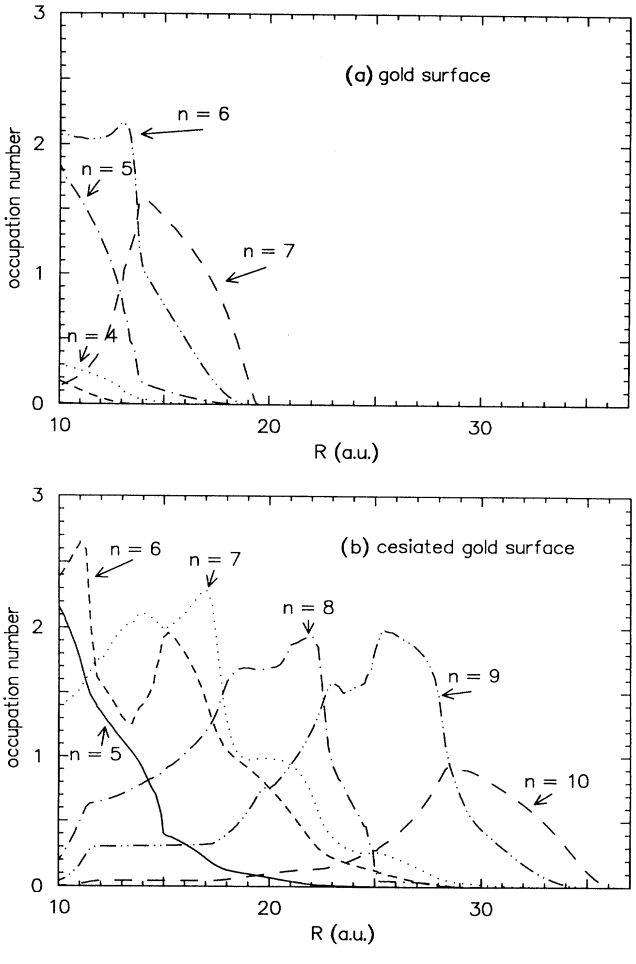

FIG. 4. Population of n shells in N^{6+} as a function of above-surface distance for (a) a clean gold surface, and (b) a cesiated gold surface ($W = 0.1$ a.u., $v_\perp = 5\times10^{-3}$ a.u.).

offset the gain in available relaxation time.

Instead, the dominant effect of the work-function reduction on the above-surface K Auger yields is the suppression of the image acceleration for the ion in front of the cesiated surface at large distances due to the screening by the charge cloud of electrons already captured in outer shells ($n=8-10$). Despite the fact that the electrons populating those outer shells of the hollow atom do not rapidly relax towards the L shell, they are nevertheless very effective in screening the ionic charge of N^{6+}, thereby reducing the gain in perpendicular speed due to the image acceleration. Figure 5 shows simulation results for the projectile energy gain resulting from image-potential acceleration during the above-surface neutralization as a function of surface work function for the same model parameters as those used to obtain the results shown in Figs. 3 and 4. Also shown in the figure are results obtained using the simple staircase model described in Ref. [17]. As can be seen, both the full simulation and the simplified model predict almost a factor of 2 decrease in energy gain over the range of work functions investigated. It is this mechanism which leads to an increase of the interaction time during the later stages of the autoionization cascade (occurring within roughly $8a_0$ of the surface and involving shells with $n \leq 4$). For the same reason, the fractional enhancement of the K Auger emission by cesiation is only weakly dependent upon the model for the electronic structure. The key parameter is the distance for the onset of neutralization $R_c(W)$, where the image acceleration becomes suppressed by resonant charge transfer.

The discrepancy between experiment and simulation at the smallest perpendicular velocities is at present not completely understood. One factor that might limit above-surface K Auger emission prematurely at the extreme grazing-incidence conditions investigated in the present work is surface flatness. However, the above-surface yields obtained for "clean" Au are, if anything, larger than those quoted by Das and Morgenstern [5] for a clean Ni(011) target, who, using decelerated beams, reached similar perpendicular velocities at significantly steeper incidence angles, where surface flatness is less of an issue. Nevertheless, target-to-target variations do appear possible, and may explain the significantly larger above-surface yields we obtained with our present "clean" Au sample as compared to our earlier Au and Cu results [7]. In addition, we cannot exclude the possibility of nonuniform Cs deposition. While some auxiliary measurements were made to verify that the electron spectra obtained were independent of ion-beam-impact location on the surface, we cannot be certain that the target site at which our work-function measurements were made coincided with that at which our multicharged ion-induced electron spectra were measured.

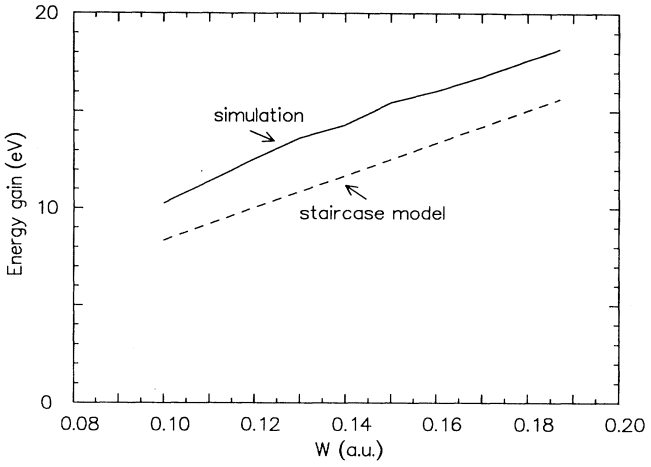

FIG. 5. Simulation results for the projectile energy gain experienced by N^{6+} ions due to image-potential acceleration, as a function of surface work function W. The staircase model results also shown are described in Ref. [17].

The following shortcomings of the simulation should be considered as well: the calculation does not take into account modifications of the dielectric response, and hence, image interaction, due to the Cs overlayer. Furthermore, for a cesiated surface the criterion of slow parallel projectile velocities $v_{\parallel}$ compared to the target Fermi velocity v_F, required for neglecting effects of the Galilei transformation of the electronic band structure relative to the moving projectile [18] is no longer satisfied.

ACKNOWLEDGMENTS

This research was supported by the Division of Applied Plasma Physics, Office of Fusion Energy, and by the Division of Chemical Sciences, Office of Basic Energy Sciences of the U.S. Department of Energy, under Contract No. DE-AC05-84OR21400 with Martin Marietta Energy Systems, Inc., and by the National Science Foundation. L.F. and I.G.H. were supported by the Oak Ridge National Laboratory through a program administered by the Oak Ridge Institute for Science and Education.

[1] J. Burgdörfer, P. Lerner, and F. W. Meyer, Phys. Rev. **44**, 5674 (1991).

[2] M. Schulz, C. Cocke, S. Hagmann, M. Stöckli, and H. Schmidt-Böcking, Phys. Rev. A **44**, 1653 (1991).

[3] H. J. Andrä, A. Simionovici, T. Lamy, A. Brenac, G. Lamboley, J. J. Bonet, A. Fleury, M. Bonnefoy, M. Chassevent, S. Andriamonje, and A. Pesnelle, Z. Phys. D Suppl. **21**, S135 (1991).

[4] F. W. Meyer, S. H. Overbury, C. C. Havener, P. A. Zeijlmans van Emmichoven, and D. M. Zehner, Phys. Rev. Lett. **67**, 723 (1991).

[5] J. Das and R. Morgenstern, Phys. Rev. A **47**, R755 (1993).

[6] B. d'Etat, J. P. Briand, G. Ban, L. de Billy, J. P. Desclaux, and P. Briand, Phys. Rev. A **48**, 1098 (1993).

[7] F. W. Meyer, S. H. Overbury, C. C. Havener, P. A. Zeijlmans van Emmichoven, J. Burgdörfer, and D. M. Zehner, Phys. Rev. A **44**, 7214 (1991).

[8] H. Winter, Europhys. Lett. **18**, 207 (1992).

[9] H. Kurz, K. Töglhofer, HP. Winter, F. Aumayr, and R. Mann, Phys. Rev. Lett. **69**, 1140 (1992).
[10] J. Das, L. Folkerts, and R. Morgenstern, Phys. Rev. A **45**, 4669 (1992).
[11] S. Schippers, S. Husted, W. Heiland, R. Köhrbrück, J. Bleck-Neuhaus, J. Kemmler, D. Lecler, and N. Stolterfoht, Nucl. Instrum. Methods B **78**, 106 (1993).
[12] J. P. Briand, L. de Billy, P. Charles, S. Essabaa, P. Briand, R. Geller, J. P. Desclaux, S. Bliman, and C. Ristori, Phys. Rev. Lett. **65**, 159 (1990).
[13] M. Schottke-Klein, A. Böttcher, R. Imbeck, S. Kennou, A. Morgante, and G. Ertl, Thin Solid Films **203**, 131 (1991).
[14] T. Gustafsson, private communication.
[15] F. W. Meyer, C. C. Havener, and P. A. Zeijlmans van Emmichoven, preceding paper, Phys. Rev. A **48**, 4476 (1993).
[16] H. P. R. Frederikse and H. D. Hagstrum, in *AIP Physics Vade Mecum,* edited by Herbert Anderson (AIP, New York, 1981), pp. 290 and 309.
[17] J. Burgdörfer and F. W. Meyer, Phys. Rev. A **47**, R20 (1993).
[18] J. Burgdörfer, E. Kupfer, and H. Gabriel, Phys. Rev. A **35**, 4963 (1987).